



Article

Integrated Geological, Hydrogeological, and Geophysical Investigations of a Barchan Sand Dune in the Eastern Region of Saudi Arabia

Mohammed Benaafi ^{1,*}, Sherif M. Hanafy ², Abdullatif Al-Shuhail ² , Ammar El-Husseiny ²  and Jack Dvorkin ²

¹ Center for Environment and Water, King Fahd University of Petroleum & Minerals, Dhahran 34464, Saudi Arabia

² College of Petroleum Engineering and Geosciences, King Fahd University of Petroleum & Minerals, Dhahran 34464, Saudi Arabia; sherif.mahmoud@kfupm.edu.sa (S.M.H.); ashuhail@kfupm.edu.sa (A.A.-S.); ammar.elhusseiny@kfupm.edu.sa (A.E.-H.); jack.dvorkin@kfupm.edu.sa (J.D.)

* Correspondence: benaafi@kfupm.edu.sa

Received: 15 January 2020; Accepted: 25 February 2020; Published: 2 March 2020



Abstract: In arid countries such as Saudi Arabia, aeolian sand often covers a large area of the country. Understanding the variations of sand properties in dunes, including grain size, sorting, mineral composition and water content, can be important for groundwater recharge, environmental, and construction applications. Earlier studies examined properties of sand dunes by collecting samples from the surface. This study aims to investigate variations of sand properties within a Barchan sand dune in the coastal area of Saudi Arabia, by collecting samples and measurements from two vertically drilled boreholes up to the ground water level; one drilled in the dune crest and another one in the limb. Representative samples were collected and analyzed for their texture parameters, water content, and mineralogy. Electrical resistivity survey data was also acquired to map water content variation in the dune limb, and for comparison with well bore data. The reported results show no vertical variations in grain size or sorting in the dune crest. In contrast, the upper 0.5 m of the dune limb shows a relatively poorer sorting than found in deeper parts of the dune. Laterally, no variations in mineralogy were observed between crest and limb sands while grain size tended to be slightly coarser in the dune limb compared to the crest. Regarding the water content, it was found to vary vertically, probably due to previous cycles of rainfall infiltration through the sand body. Such observed variation in water content is consistent with the measured resistivity profile which could clearly identify the water table and areas with higher water content. This study concludes that beyond the upper 0.5 m, the Barchan sand dune body can be treated as a homogeneous medium in terms of mineralogy and sorting while grain size increases slightly toward the limb side.

Keywords: Barchan sand dune; Saudi Arabia; electrical resistivity; vadose zone; sand moisture; hydrogeology

1. Introduction

More than one-third of Saudi Arabia is covered by aeolian sand dunes in four large dune fields, namely, Ar Rub' al Khali, An Nafud, Ad Dahna, and Al Jafurah [1]. In the Eastern Province of Saudi Arabia, the sand dunes that occurred in the coastal area belong to the Al Jafurah dune field, which lies south of the Gulf of Bahrain [1]. The aeolian sand in the Eastern Province was accumulated during the Quaternary Period and originated from the Bitlis–Zagros thrust belt [2]. Its source was the Tigris–Euphrates paleo-river system. Sands were transported by northerly winds (Shamal) during the Pleistocene Period and formed barchanoid dunes due to the consistent high speed of the winds [3,4].

The sand dunes of the Al Jafurah desert are younger than other dunes in Arabia. Their sand was accumulated 4000 years ago [5].

According to the previous studies, the sand dunes in the Eastern Province of Saudi Arabia display variability in terms of texture and composition that are controlled by the geographic location [1–6]. The reported range of grain size and sorting is from fine to coarse, and poorly sorted to very well sorted, respectively [2,6]. Regarding the mineral composition, the early work shows that the sand dunes located close to the Arabian Gulf coastal area consist mainly of quartz with significant amount of feldspars, and carbonate minerals [4]. No previous work was done on the water content profile of the sand dunes in the Eastern Province of Saudi Arabia. Additionally, earlier studies examined properties of sand dunes based on samples collected from the dune surface, which may not be representative of the internal sand dune body at certain depths. The vertical and lateral variation in texture, mineral composition, and water content of the sand dune is important for groundwater recharge, and environmental and construction applications. The aim of this study is to investigate the lateral and vertical variation of Barchan dune properties, including sand texture, mineral composition, and water content, by adopting an integrated approach of geological, hydrogeological, and geophysical techniques. The sand properties were measured on samples collected from two boreholes drilled in the crest and limb of a Barchan sand dune, which is located 30 km east of Dhahran city in the Eastern Province of Saudi Arabia (Figure 1). Moreover, the variation in water content of the studied sand dune was also mapped using an electrical resistivity survey. Electrical resistivity tomography (ERT) and vertical electrical sounding (VES) have been used extensively to delineate the areas of fresh and brackish water within the sand dunes [7–11].

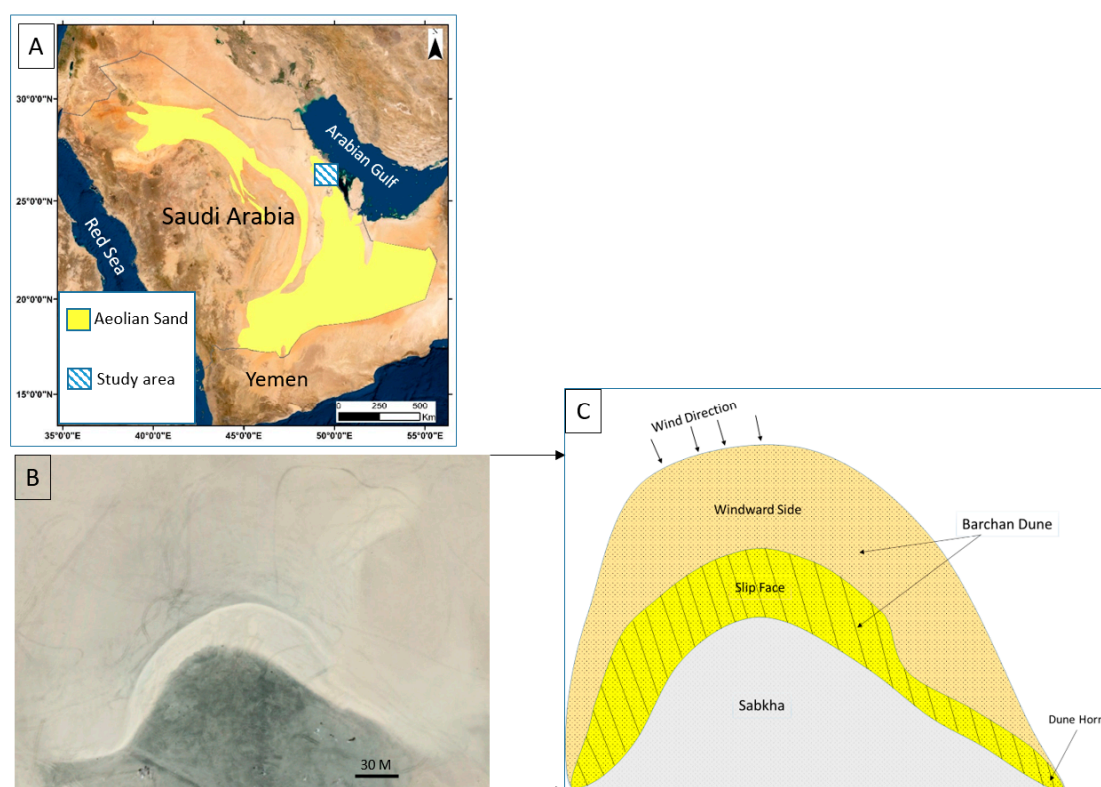


Figure 1. (A) A satellite image showing the distribution of aeolian sand in Saudi Arabia, (B) a high-resolution satellite image of the studied Barchan dune in the Eastern Province of Saudi Arabia, and (C) a schematic illustration of the studied Barchan sand dune.

2. Materials and Methods

2.1. Sand Sampling Method

The Geoprobe drilling rig, with a direct pushing hammer and rotary techniques, was used to drill two boreholes at the depth of 10 m in the Barchan sand dune in the Eastern Province of Saudi Arabia. Eighty-three undisturbed sand samples were collected from the two boreholes using the standard split spoon method. A spilt spoon, 5 cm in diameter and 70 cm in length, was lowered into the borehole after being attached to the string of the drill rod. The direct pushing hammer was used to push the split spoon into the sand dune at the bottom of the borehole. After the spoon was filled with sand, it was brought back to the surface. The sand in the split spoon was packed in glass bottles and delivered to the laboratory for further analyses.

2.2. Electrical Resistivity Tomography (ERT)

The electric resistivity method is a common geophysical technique used for many decades in geological, engineering, archaeological, mining, environmental, and groundwater applications, and sometimes it is also used in hydrocarbon exploration [12–14]. In this technique, the subsurface resistivity variations are measured from the ground surface as a function of the electrode separations [13]. Then, the true resistivity of the subsurface as a function of depth can be calculated accordingly.

ERT, as a two-dimensional (2-D) modeling technique, was used to find the resistivity changes in the vertical and horizontal directions along the survey line. Here, we assumed that the resistivity is constant in the direction perpendicular to the survey line, which is a valid assumption in many geological situations [12,15].

In practice, four electrodes are required for the field measurements. Two of these four electrodes (called C1 and C2) are used to inject the current (I) into the subsurface and the other two electrodes (called P1 and P2) are used to measure the potential difference (ΔV). Then, the apparent resistivity (ρ_a) measured in (Ohm-m) is calculated by (e.g., [14]):

$$\rho_a = k \frac{\Delta V}{I}, \quad (1)$$

$$k = \frac{2\pi}{\left(\frac{1}{r_{C_1P_1}} - \frac{1}{r_{C_2P_1}} - \frac{1}{r_{C_1P_2}} + \frac{1}{r_{C_2P_2}} \right)} \quad (2)$$

where k is a geometrical factor measured in meters that depends on the electrode spread, and $r_{C_1P_1}$ is the distance between the current electrode (C1) and the potential electrode (P1). In this field example we used two electrode spreads:

1. Wenner spread (Figure 2a). This is a commonly used electrode spread in field measurements. In this spread the electrodes are uniformly spaced in a line with the offset between each two successive electrodes equal to ' a '. In this case, the geometrical factor ' k ' in Equation (2) is reduced to $k = 2\pi a$.
2. Schlumberger spread (Figure 2b). The current electrodes in this spread are spaced much further apart than the potential electrodes, where the offset between the current electrodes is equal to ' $2L$ ' and the offset between the potential electrodes is equal to ' $2l$ '. Here, the geometrical factor ' k ' in Equation (2) is reduced to $k = \frac{2\pi l^2}{2l}$; for more details see [16].

For depth exploration, the offsets between the electrodes are gradually expanded about a fixed point, while for lateral exploration and mapping the offsets between the electrodes remain constant and all four electrodes are moved along the profile. In this field example we used two common electrode spreads, Wenner and Schlumberger, to increase the resolution of the subsurface model [13–16].

In this study, we recorded an ERT profile using 96 electrodes with 0.75 m electrode intervals arranged on the top of the sand dune at the limb side. All electrodes were connected to the measuring

unit using a multi-core cable and the electric switching unit was used to automatically select the relevant four electrodes for each measuring point. The recorded apparent resistivity was then inverted to obtain the true resistivity as a function of depth.

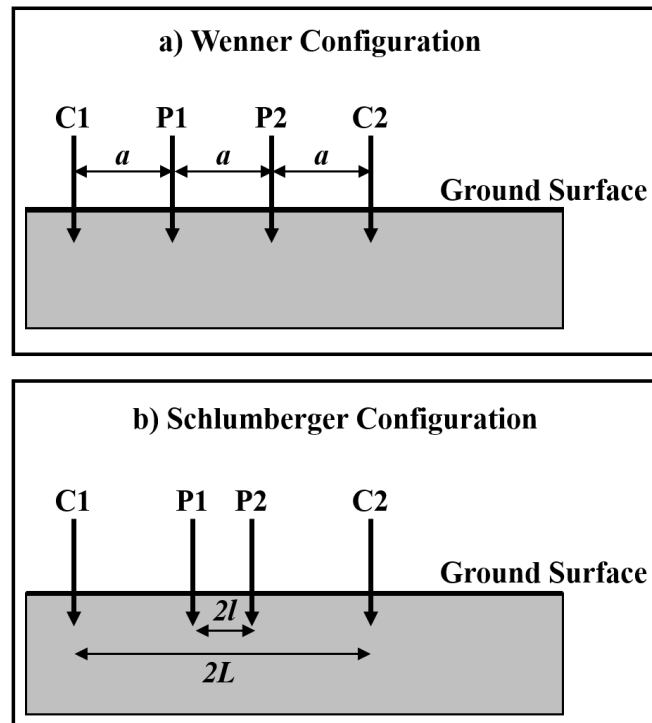


Figure 2. The two spreads used in the field recording, (a) Wenner and (b) Schlumberger spreads. C1 and C2 are the two current electrodes while P1 and P2 are the potential electrodes. The offset between any two successive electrodes in the Wenner spread is 'a'; the offsets between the two current and the two potential electrodes in the Schlumberger spreads are '2L' and '2l', respectively.

2.3. Laboratory Analyses

2.3.1. Water Content

The water content of the sand samples collected from the unsaturated part of the studied Barchan dune was measured in the laboratory using the gravimetric method with oven-drying. The sand samples were kept in a glass bottle after being retrieved from boreholes, and the weight was recorded on-site. The collected samples were immediately shipped to the laboratory, where they were dried in the oven at 105 °C for 48 h. The sample weight was recorded after oven-drying, and the water content of sand samples was then calculated as the percentage of the mass of water per mass of the dried sand sample.

2.3.2. Salinity

The salinity of the collected sand samples was obtained by measuring the electrical conductivity of water extracted from the sand sample by mixing 50 g of each sample with 50 mL of deionized water. The electrical conductivity probe was used to measure the electrical conductivity of the sand samples.

2.3.3. Grain Size Distribution

The grain size distribution of the collected sand samples was obtained using a laser diffraction particle size analyzer. The statistical parameters of the grain size (i.e., mean grain size and sorting) were calculated based on the grain size cumulative curves [17].

2.3.4. Mineral and Chemical Composition

The X-ray powder diffraction technique was used to quantify the mineral composition of the collected sand samples. In addition, the bulk elemental composition of the tested sand samples was obtained using the micro X-ray fluorescence technique.

3. Results

3.1. Lithology of the Sand Dune

Two lithology logs of the studied Barchan dune were established using the data collected from the two boreholes, as shown in Figure 3. The 10 m borehole (Borehole n°2) that was drilled into the dune crest (along the windward side) consisted of fine- to medium-grain sands (Figure 3). It did not reach the water table. On the other hand, the 10 m borehole (Borehole n°1), which was drilled in the dune limb (horn), penetrated 7 m of the medium-grained sand (the sand dune), followed by 2.5 m of fine- to medium-grain sandy sabkha and 0.5 m of clay-sandy sabkha (Figure 3). The water table was found below the sand dune in the sabkha section, 7.6 m below the ground surface.

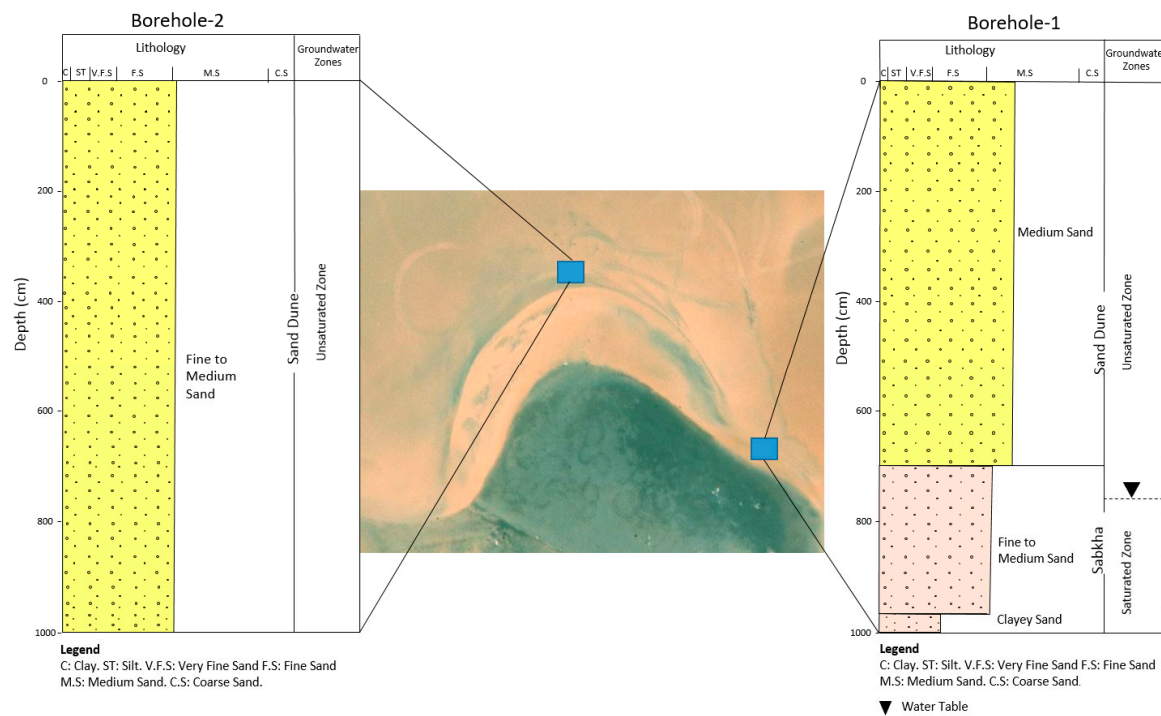


Figure 3. Lithology logs of the two boreholes showing the sand type and groundwater zones.

3.2. Mineral Composition of Sands

The bulk mineral composition of the collected sand samples was found to include quartz, feldspars, and calcite as the major minerals, and gypsum and heavy minerals as the minor ones (Figure 4). The reported values of quartz, feldspars, calcite, heavy minerals were 86.8%, 9.4%, 2.9% and 0.9%, respectively. Similar mineral compositions were observed at the sand dune crest and the sand dune limb, indicating the same source of sand grains for both areas.

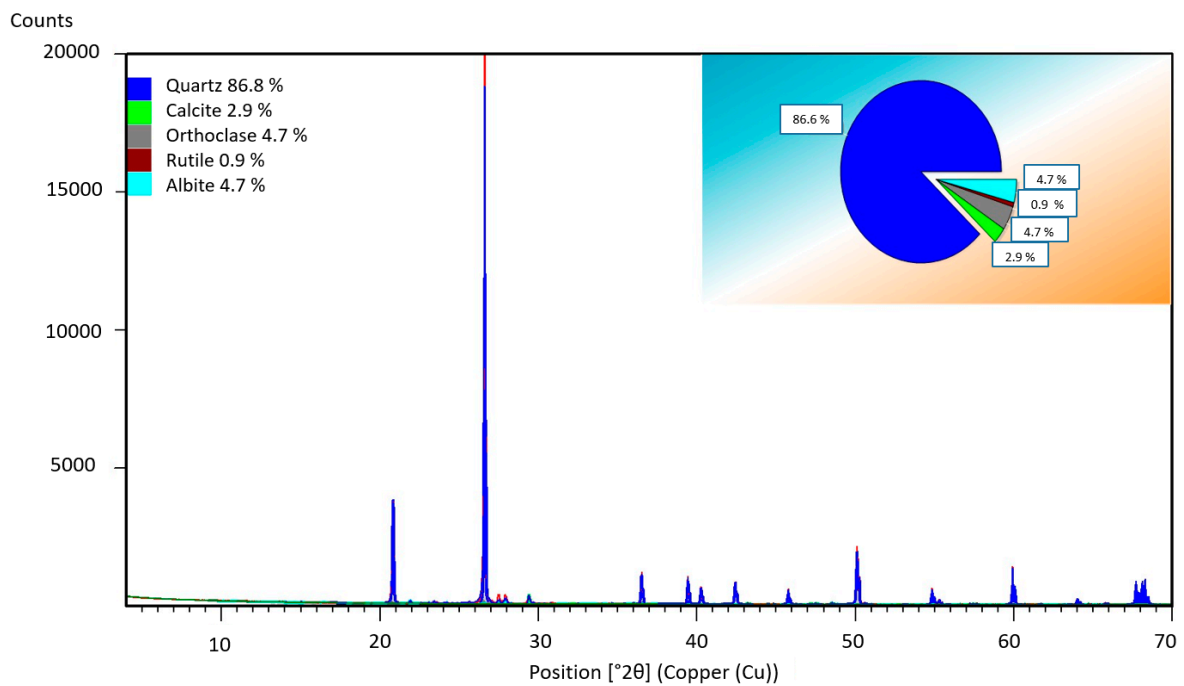


Figure 4. X-ray powder diffraction chart showing the mineral composition of the studied sand dune.

3.3. Water Content

As shown in Figure 5, the water content profiles of the two boreholes (at the dune crest and dune limb) were established. In the dune limb, the last sample was collected from a depth of 650 cm beneath the ground surface owing to the presence of the water table just below. The water content varied vertically with the maximum values of 3.72% and 3.31% in the dune limb and dune crest, respectively. Although both dune limb and crest were subjected to the same rainfall, the water content on the limb showed only one shallow peak (about 0.5 m deep), while three peaks of water content were observed in the dune crest (at depths of 2.5 m, 4.5 m, and 7.7 m, respectively). Although both dune limb and crest were subjected to same rainfall, the water content on the limb showed only one shallow peak while the three peaks of water content were observed in the dune crest.

3.4. Sand Salinity

The studied dunes displayed a salinity range from 1500 ppm to 4500 ppm (Figure 6). The sand salinity profiles of the two studied sites are shown in Figure 6. An increase in the salinity of the sand dune was observed from the ground surface to the sand dune bottom. The vertical variation in the sand salinity may have been related to the leaching of evaporite minerals along the pathway of the downward movement of water in the sand dune.

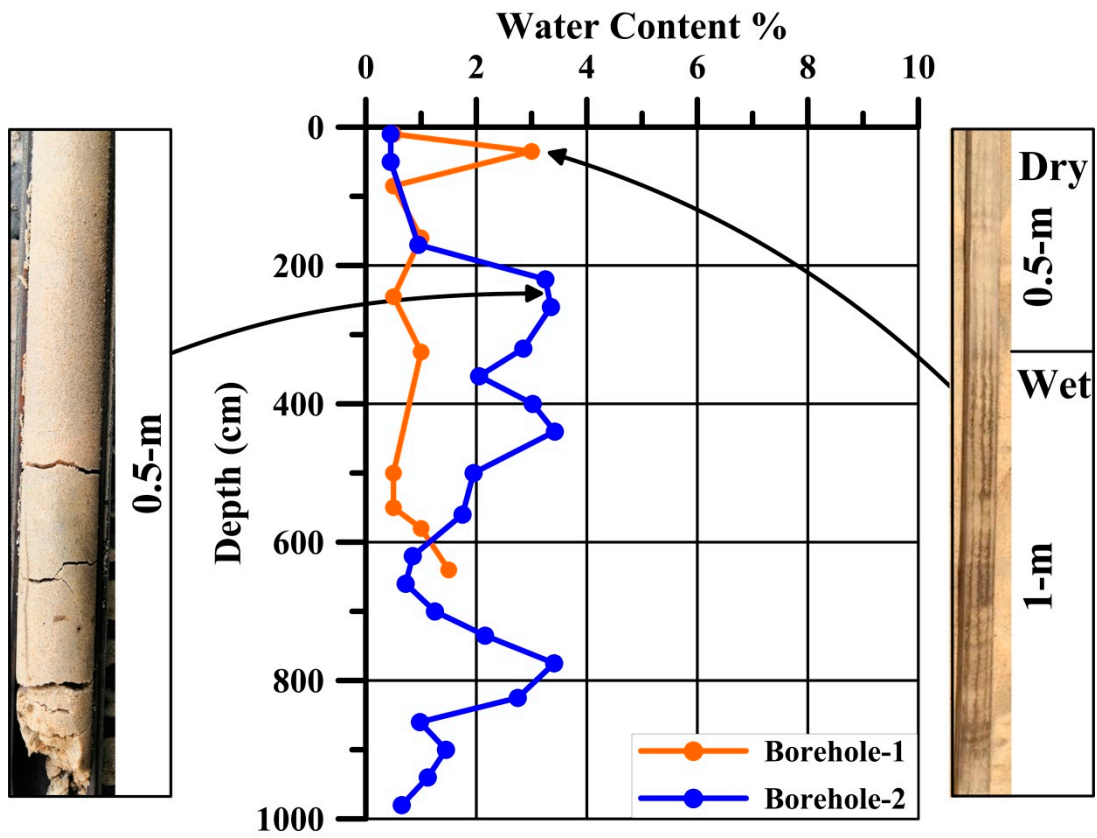


Figure 5. Water content profiles of the two boreholes.

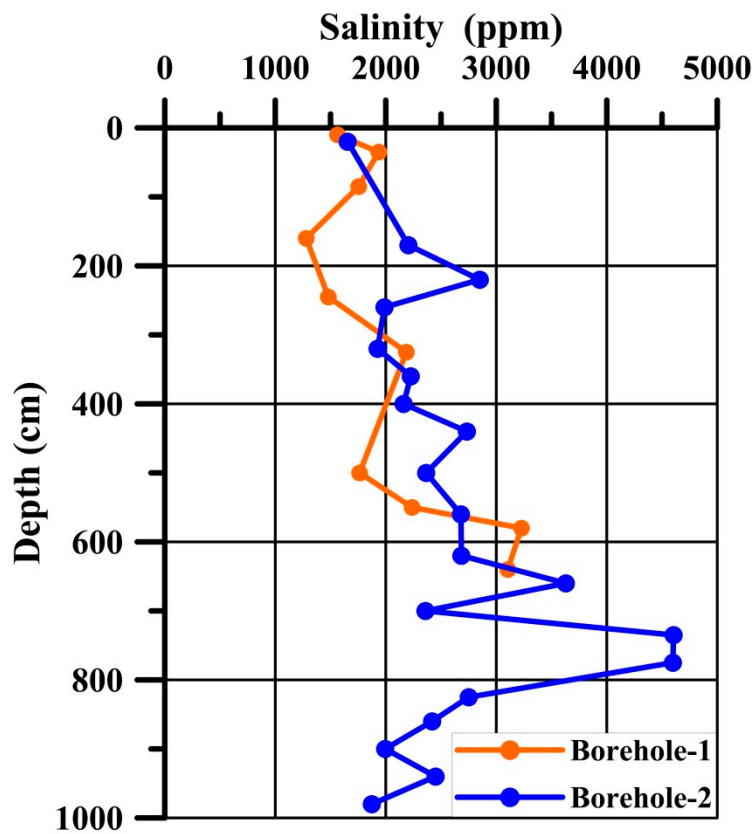


Figure 6. Sand salinity profiles of the two boreholes.

3.5. Sand Texture

Texture parameters (i.e., mean grain size, D50 (median grain size that splits the distribution into two halves), D90 (10% of the distribution has a larger size), and sorting coefficient) of the tested sand samples were measured. The result of the texture analysis revealed that the studied sand ranged from fine size (0.22 mm) to medium size (0.40 mm), as shown in Figure 7. Excluding the upper 0.5 m, the sand grains of the dune limb were found to be slightly coarser than those of the dune crest. The D50 values profiles display similarity with the mean grain size profiles calculated from the grain size cumulative curves [17] (Figure 8). The values of D90 are similar in the dune crest and limb. This occurrence indicates that the small sand grains in both sides of the dune have homogenous vertical distribution (Figure 8). The sorting coefficient of the tested sands ranged from moderately well-sorted (0.54 Phi) to poorly sorted (1.07 Phi) as shown in Figure 9. No clear vertical variation in sand sorting was observed within the sand crest down to 650 cm, while the upper 250 cm of the sand limb showed poorly sorted sand, and the lower 350 cm of the dune crest showed alternated layers of poorly and better-sorted sand (Figure 9). Between 250 cm and 650 cm, both the dune limb and crest showed a similar degree of sorting. This indicates that the mechanism of sand deposition and accumulation is the same in all parts of the studied Barchan sand dune.

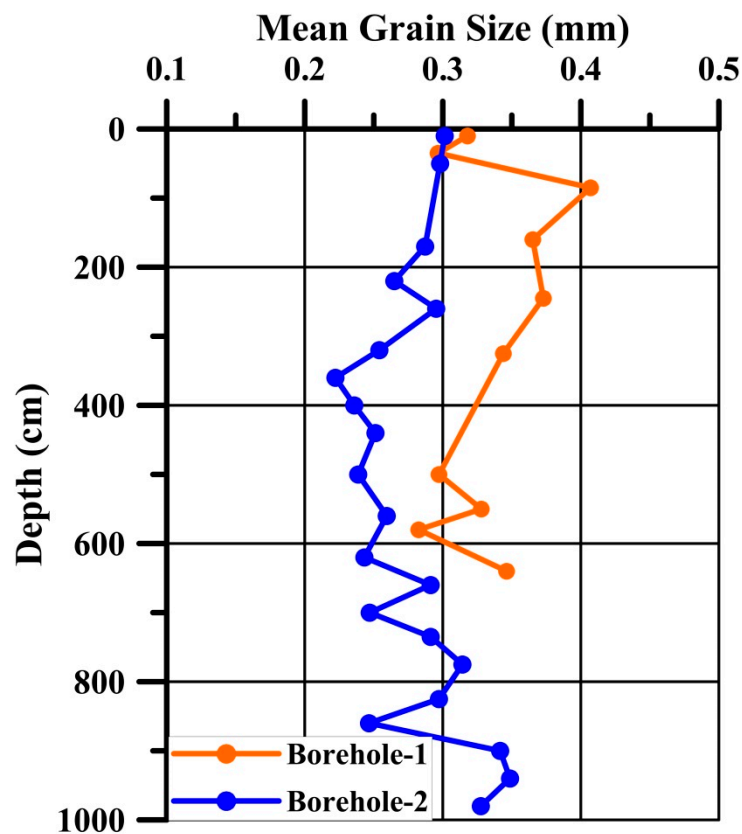


Figure 7. Mean grain size profiles of the two boreholes.

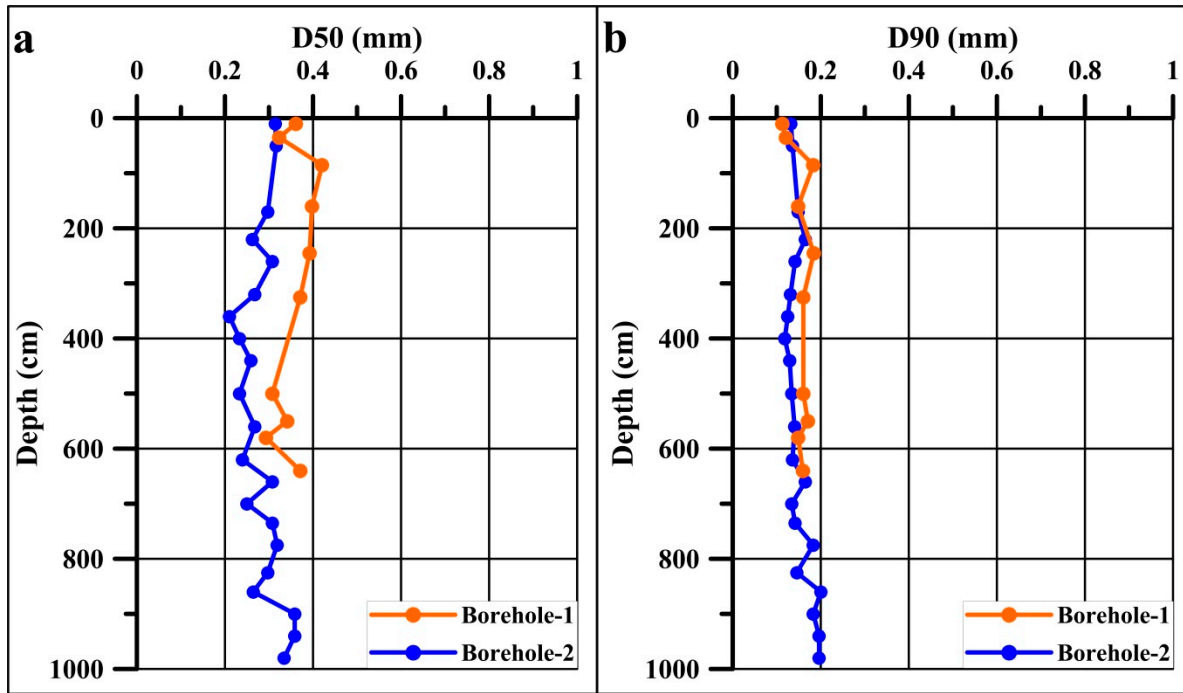


Figure 8. (a) D50 and (b) D90 of grain size distribution of the two boreholes.

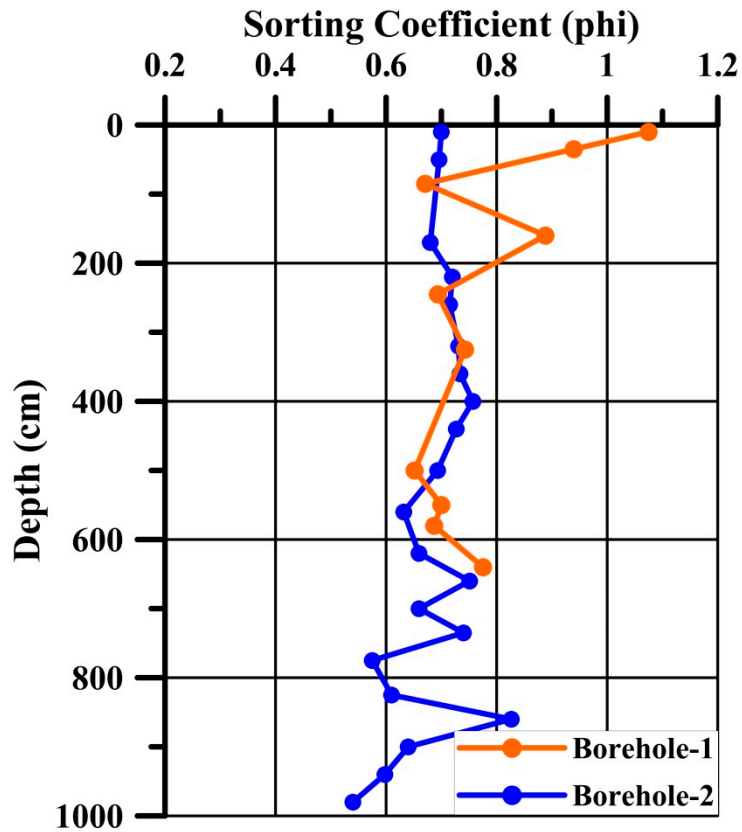


Figure 9. Sand grains sorting profiles of the two boreholes.

3.6. Electrical Resistivity Results

The recorded apparent resistivity data were inverted to obtain the ERT as shown in Figure 10. The true resistivity was between 4 Ohm-m and 1470 Ohm-m. The ERT can be divided into four zones as follows:

- Zone 1: This zone shows high resistivity values (~660 Ohm-m) at the shallow depth (0 to 0.6 m). High values are associated with the dry sand on the top of the dune.
- Zone 2: The resistivity decreases to about 170 Ohm-m at a depth between 0.6 m and 1.3 m, and is marked as “A” in Figure 10. This low-resistivity zone is associated with high water content as shown in Figure 5, due to the infiltrated rainwater from the last precipitation event, and it is vertically-shifted down in the ERT section.
- Zone 3: At a depth ranging from 2.5 m to 5.8 m, the resistivity increases to 1300 Ohm-m, and is marked as “B” in Figure 10. This corresponds to the dry sand.
- Zone 4: Finally, the resistivity gradually decreases until reaching 4.6 Ohm-m at the bottom of the ERT section. This is due to the effects of the saline groundwater and the sabkha layer.

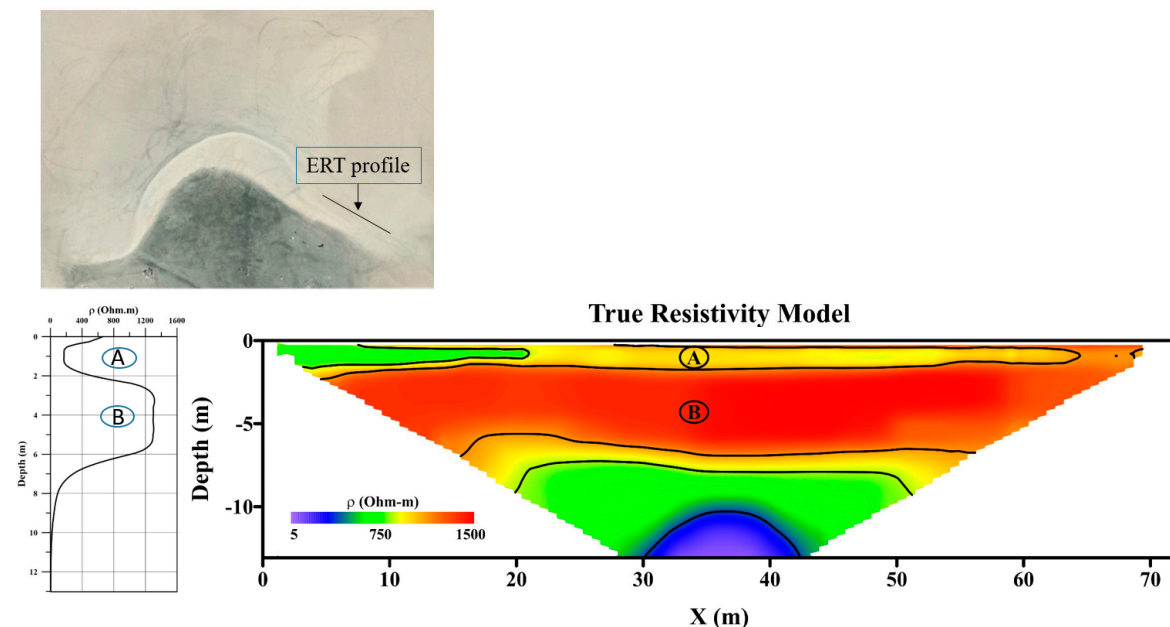


Figure 10. Electric resistivity tomogram (ERT) and resistivity profile of the dune limb, showing four zones of the electrical resistivity.

4. Discussion

The vertical and lateral variability in physical properties of the studied Barchan dune can have control on groundwater recharge and vegetation coverage in the study area. According to the literature, in a Barchan sand dune the size of sand grains varies with their position. In particular, the fine-grained sand tends to be accumulated in the dune crest and the medium to coarse-grained sands are retained in the toe of the dune windward side and dune limb (horn) [18–21]. In this regard, the findings of this study are in line with previous works. The accumulation of sand with varied sizes within different sub-environments of the Barchan dune is controlled by action of the wind that passes over and around the dune. The coarse grains move slowest and concentrate in the marginal areas of the Barchan dune, whereas the fine grains are transported faster and accumulate in the dune crest. Examining the vertical variations of sand properties, no vertical variations in grain size or sorting was observed in the crest, except the lower 350 cm display alternated poorly and well sorted sand. In contrast, samples collected from the upper 0.5 m of the dune limb show a relatively poorer sorting (clear bimodal

particle size distribution) and a lower mean grain size, compared with deeper samples (Figures 7 and 9, respectively). This suggests that samples collected from the dune surface could be representative for the internal dune body in the crest but not within the limb. The reported poorly sorted sand in the upper 0.5 m layer of the dune limb is apparently controlled by the fluctuations in wind velocity as wind moves around the sand dune. Overall, beyond the upper 0.5 m, the Barchan sand dune body can be treated as a homogeneous medium in terms of mineralogy and sorting. Such homogeneity in sand texture indicates continuity in the depositional mechanisms of sand in the studied Barchan dune through consistent northerly (Shamal) winds that deliver sand to such dune.

As has been reported in literature, the mineral composition of sand dunes in the Eastern Province of Saudi Arabia consists mainly of quartz, feldspars, and carbonate minerals [4]. Previous works identified mineral composition of sand samples collected from the dune surface; however, in this study the vertical variation in mineral composition of the studied Barchan dune was investigated. The result shows no significant change in the mineral composition of the studied dune with depth, indicating that the source of the sand and transport/sedimentation mechanisms have not varied over time.

The variability in water content of sand dunes is controlled by several factors including sand texture, dune topography, and vegetation [22–24]. Previous studies focused on the distribution of water content in sand dunes at shallow depth [25,26]. In this study, the water content of the dune was measured down to the deepest investigated deposits (i.e., –6.5 m in the dune limb, and –10 m in the dune crest). The water content profiles (Figure 5) show vertical variability: only one peak is observed in the upper part of the dune limb, while three peaks exist at major depths in the dune crest. The multiple peaks for water content could be related to multiple rainfall events. Note the presence of a wet zone in the upper 0.5 m of the limb; wet zones are instead found at major depths in the dune crest (Figure 5), suggesting that water infiltration is faster in the dune crest. This might be explained by the better sand sorting in the upper 0.5 m of the crest compared with the limb. Such better sorting can result in larger pore sizes, and thus better hydraulic conductivity of the upper part within the dune crest compared to the limb. Consequently, in the limb the rainfall infiltration seems to be slowed down and trapped in the upper poorly sorted grains, which could make it more prone to evaporation by impact of sunlight and wind as water is trapped near surface. Additionally, the sand body is thicker within the dune crest compared to the limb, and thus the infiltrated water within the dune crest is more protected from the impact of external factors (sunlight and wind) compared to the dune limb. In summary, the smaller water content in the limb could be explained by the poorly sorted sand near the surface and the thinner sand body in the limb compared to the crest. This means that the vadose zone within the dune crest is expected to have higher water saturation in the rainy season compared to the dune limb.

5. Conclusions

This study investigated variations of sand properties within a Barchan sand dune in the coastal area in the Eastern Province, Saudi Arabia, by collecting samples and measurements from two vertically drilled boreholes up to the ground water level. Such study is the first of its kind as it investigates the sand dune internal properties as a function of depth through two vertical profiles, one drilled in the dune crest and another one in the limb. The collected samples were analyzed for their grain size, sorting, water content, salinity, and mineralogy. Electrical resistivity was also acquired at the top of the dune to map water content variation and for comparison with well bore data. Our results showed no variation in mineralogy between the two vertical profiles drilled in the crest and limb. No vertical variations in grain size or sorting was observed in the dune crest and limb, in depth ranges from 250 cm to 650 cm. In contrast, the upper 250 cm of dune limb, and the lower 350 cm of dune crest, showed variability in sand sorting. The outcomes of this study suggest that samples collected from the dune surface could be representative for the internal dune body in the crest but not within the limb. When comparing the crest with limb (excluding the upper 0.5 m data), grain size tends to be relatively larger in the limb while a similar degree of sorting is observed between both vertical

profiles. The relatively coarser grain size in the limb might be explained by the topographic differences (dune slope and height). The wind, as the main carrier of sand grains, transports the fine grains up to dune crest while leaving the coarser ones in the dune marginal area. Regarding the water content, it was found to vary vertically and laterally throughout the dune body. The vertical variations could be explained by multiple rainfall events while the larger water content in the dune crest might be due to variations in the sorting of sand within the upper 50 cm between the dune crest and limb. The observed vertical variation in water content is consistent with the measured resistivity profile which could clearly identify the water table and areas with higher water content. The textural and mineralogical homogeneity and the low salinity of the studied dune increase its role to recharge the shallow aquifer in the study area with freshwater.

Author Contributions: All authors contributed in this manuscript and their contributions specified as following: M.B. contributed in writing the original draft preparation, conceptualization, investigation, methodology and data curation; S.M.H. participated in writing the original draft preparation, methodology and data curation. A.A.-S. has contribution in writing the original draft preparation, conceptualization, methodology, and supervision, project administration, and funding acquisition; A.E.-H. contribute in data curation, writing—review and editing, and investigation; J.D. participate in conceptualization and supervision. All authors have read and agreed to the published version of the manuscript.

Funding: This research was funded by the College of Petroleum Engineering & Geosciences at KFUPM, grant number SF18060.

Acknowledgments: The College of Petroleum Engineering & Geosciences at KFUPM is acknowledged for support and assistance provided for field and laboratory studies under Start-Up Project No. SF18060.

Conflicts of Interest: The authors declare no conflicts of interest.

References

1. Edgell, S. *Arabian Deserts: Nature, Origin and Evolution*; Springer: Dordrecht, The Netherlands, 2006; pp. 1–644.
2. Anton, D. Modern eolian deposits of the eastern province of Saudi Arabia. *Dev. Sedimentol.* **1983**, *38*, 365–378.
3. Fryberger, S.G.; AL-SARI, A.M.; Clisham, T.J.; Rizvi, S.A.; AL-HINAI, K.G. Wind sedimentation in the Jafurah sand sea, Saudi Arabia. *Sedimentology* **1984**, *31*, 413–431. [[CrossRef](#)]
4. Garzanti, E.; Vermeesch, P.; Andò, S.; Vezzoli, G.; Valagussa, M.; Allen, K.; Kadi, K.A.; Al-Juboury, A.I. Provenance and recycling of Arabian desert sand. *Earth-Science Rev.* **2013**, *120*, 1–19. [[CrossRef](#)]
5. Anton, D.; Vincent, P. Parabolic dunes of the Jafurah desert, eastern province, Saudi Arabia. *J. Arid Environ.* **1986**, *11*, 187–198. [[CrossRef](#)]
6. Benaafi, M.; Abdullatif, O. Sedimentological, mineralogical, and geochemical characterization of sand dunes in Saudi Arabia. *Arab. J. Geosci.* **2015**, *8*, 11073–11092. [[CrossRef](#)]
7. Lebbe, L.C. Mathematical model of the evolution of the fresh water lens under the dunes and beach with semi-diurnal tides. in 8th salt water intrusion meeting, Bari. *Geol. Appl. Idrogeol.* **1983**, *18*, 211–226.
8. Greggio, N.; Giambastiani, B.; Balugani, E.; Amaini, C.; Antonellini, M. High-Resolution Electrical Resistivity Tomography (ERT) to Characterize the Spatial Extension of Freshwater Lenses in a Salinized Coastal Aquifer. *Water* **2018**, *10*, 1067. [[CrossRef](#)]
9. Newton, B.T.; Allen, B. *Hydrologic Investigation at White Sands National Monument*; Aquifer Mapping Program; New Mexico Bureau of Geology and Mineral Resources: Socorro, NM, USA, 2014; Available online: https://geoinfo.nmt.edu/publications/openfile/downloads/500-599/559/OFR559_White_Sands_with_Appendices_LR.pdf (accessed on 27 February 2020).
10. Kowalczyk, S.; Żukowska, K.A.; Mendecki, M.J.; Łukasiak, D. Application of electrical resistivity imaging (ERI) for the assessment of peat properties: A case study of the Całowanie Fen, Central Poland. *Acta Geophys.* **2017**, *65*, 223–235. [[CrossRef](#)]
11. Groen, M.; Kok, A.; van der Made, K.J.; Post, V.E.A. The use of mapping the salinity distribution using geophysics on the island of Terschelling for groundwater model calibration. In Proceedings of the 20th Salt Water Intrusion Meeting, Naples, FL, USA, 23–27 June 2008.
12. Loke, M.H.; Chambers, J.E.; Rucker, D.F.; Kuras, O.; Wilkinson, P.B. Recent developments in the direct-current geoelectrical imaging method. *J. Appl. Geophys.* **2013**, *95*, 135–156. [[CrossRef](#)]

13. Hanafy, S.M. Mapping the Qademah fault with traveltime, surface-wave, and resistivity tomograms. In *SEG Technical Program Expanded Abstracts*; SEG: New Orleans, LA, USA, 2015; pp. 3347–3351.
14. Hanafy, S.M.; Jonsson, S.; Klinger, Y. Imaging normal faults in alluvial fans using geophysical techniques: Field example from the coast of Gulf of Aqaba, Saudi Arabia. In *SEG Technical Program Expanded Abstracts*; SEG: Denver, CO, USA, 2014; pp. 4670–4674.
15. Loke, M.H. Electrical resistivity surveys and data interpretation. In *Solid Earth Geophysics Encyclopedia*, 2nd ed.; Springer: Berlin, Germany, 2011; pp. 276–283.
16. Zohdy, A.A.; Eaton, G.P.; Mabey, D.R. *Application of Surface Geophysics to Ground-Water Investigations; Techniques of Water-Resources Investigations*, USGS: Reston, VA, USA, 1974; 116p. [[CrossRef](#)]
17. Folk, R.L.; Ward, W.C. A Study in the Significance of Grain-Size Parameters. *J. Sediment. Petrol.* **1957**, *27*, 3–26. [[CrossRef](#)]
18. Folk, R.L. Genesis of longitudinal and oghurd dunes elucidated by rolling upon grease. *Geol. Soc. Am. Bull.* **1971**, *82*, 3461–3468. [[CrossRef](#)]
19. Sidwell, R.G.; Tanner, W.F. Sand grain patterns of west Texas dunes. *Am. J. Sci.* **1939**, *237*, 181–187. [[CrossRef](#)]
20. Zhang, Z.; Dong, Z. Grain size characteristics in the Hexi Corridor Desert. *Aeolian Res.* **2015**, *18*, 55–67. [[CrossRef](#)]
21. Zhang, Z.; Dong, Z.; Hu, G.; Parteli, E. Migration and morphology of asymmetric barchans in the Central Hexi Corridor of Northwest China. *Geosciences* **2010**, *8*, 204. [[CrossRef](#)]
22. Zhang, Z.C.; Dong, Z.B. Dune field patterns and wind environments in the middle reaches of the Heihe Basin. *J. Desert Res.* **2014**, *34*, 332–341.
23. Zhang, Y.; Liu, J.; Xu, X.; Tian, Y.; Li, Y.; Gao, Q. The response of soil moisture content to rainfall events in semi-arid area of Inner Mongolia. *Procedia Environ. Sci.* **2010**, *2*, 1970–1978. [[CrossRef](#)]
24. Zhou, J.; Fu, B.; Gao, G.; Lü, N.; Lü, Y.; Wang, S. Temporal stability of surface soil moisture of different vegetation types in the Loess Plateau of China. *Catena* **2015**, *128*, 1–15. [[CrossRef](#)]
25. Wang, Z.; Wang, L.; Liu, L.; Zheng, Q. Preliminary study on the spatiotemporal distribution of moisture content in sand dunes in the southern marginal zone of the Mu Us Desert. *Arid Zone Res.* **2007**, *24*, 61–65.
26. Zhao, J.; Ma, Y.; Luo, X.; Yue, D.; Shao, T.; Dong, Z. The discovery of surface runoff in the megadunes of Badain Jaran Desert, China, and its significance. *Sci. China Earth Sci.* **2017**, *60*, 707–719. [[CrossRef](#)]



© 2020 by the authors. Licensee MDPI, Basel, Switzerland. This article is an open access article distributed under the terms and conditions of the Creative Commons Attribution (CC BY) license (<http://creativecommons.org/licenses/by/4.0/>).